Supplementary Information

Polyoxometalate-modified reduced graphene oxide foam as monolith reactor for efficient flow catalysis of epoxide ring-opening reactions

Xiaoting Jing, Zhen Li, Weijie Geng, Yingnan Chi,* Hongjin Lv,* Changwen Hu

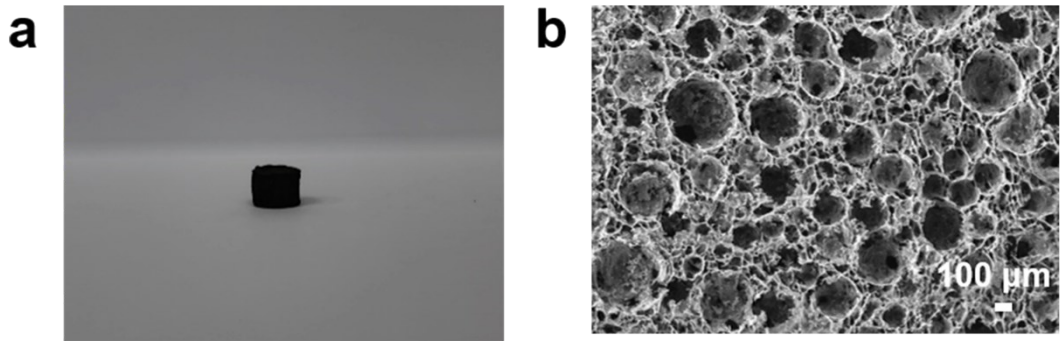

Figure S1. The (a) digital photograph and (b) SEM image of PW_{12}@rGO monolith.

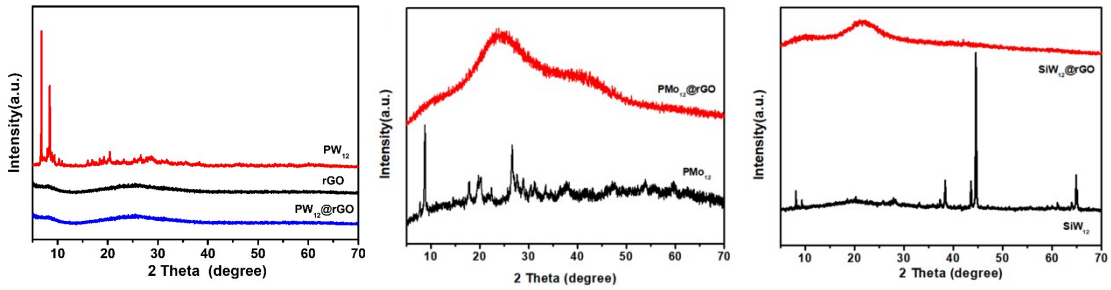

Figure S2. Powder XRD patterns of rGO, POMs, and POM@rGO composites.

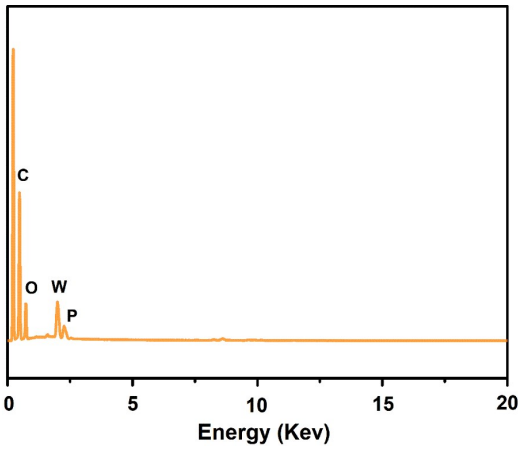

Figure S3. EDS spectra of PW_{12}@rGO.

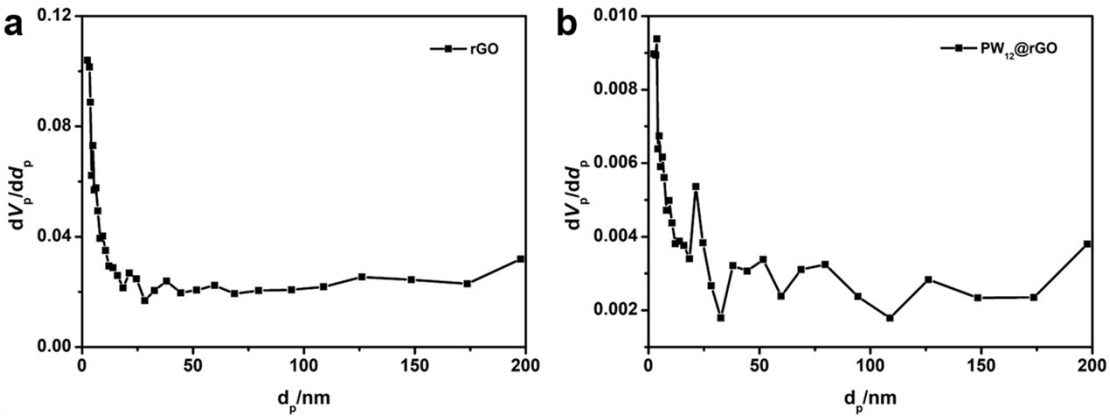

Figure S4. Pore size distributions of (a) rGO and (b) PW_{12}@rGO by BJH method desorption branch.

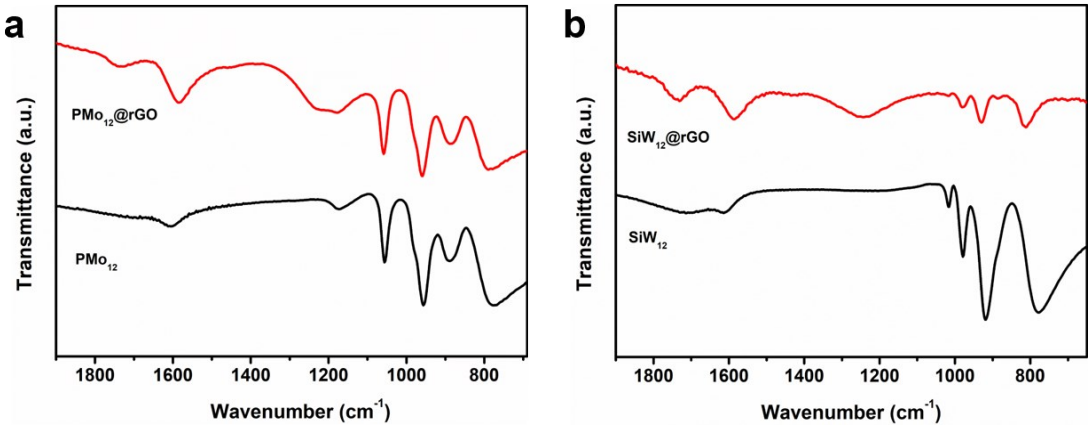

Figure S5. FT-IR spectra of PMo_{12}@rGO and SiW_{12}@rGO.

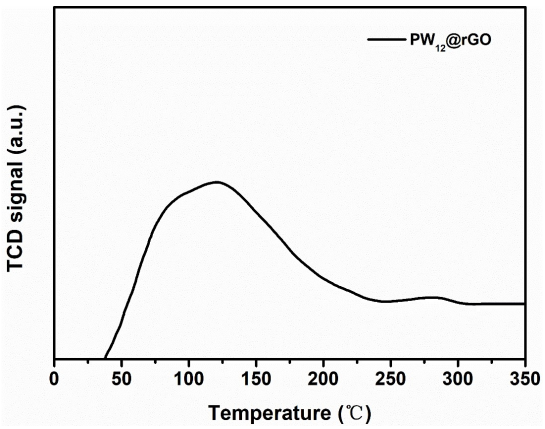

Figure S6. NH_3-TPD for PW_{12}@rGO.

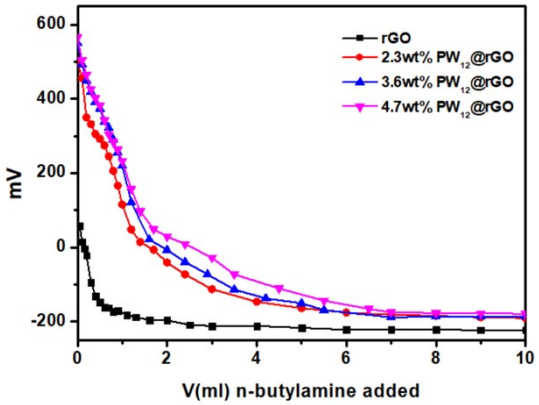

Figure S7. Potentiometric titration curves of n-butylamine in acetonitrile for different PW_{12}@rGO composites.

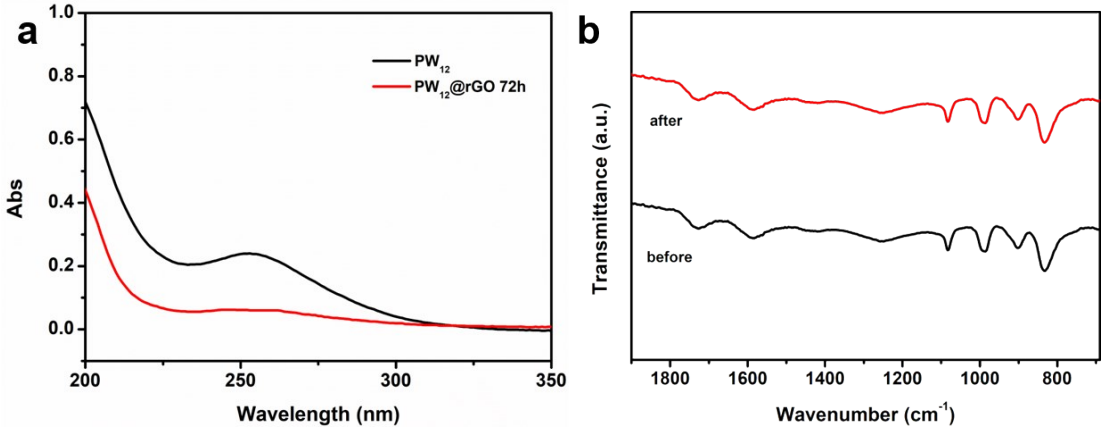

Figure S8. (a) Liquid-phase UV-vis spectra from leaching test of PW_{12}@rGO immersed in methanol for 72 h. (b) FT-IR spectra of PW_{12}@rGO before and after the leaching test.

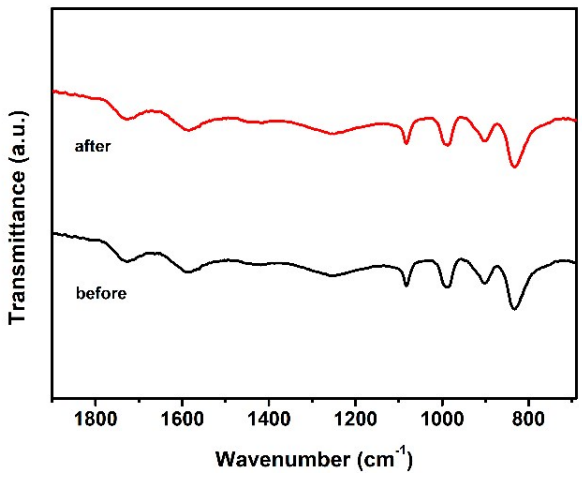

Figure S9. FT-IR spectra of recycled and fresh PW_{12}@rGO in batch reaction.

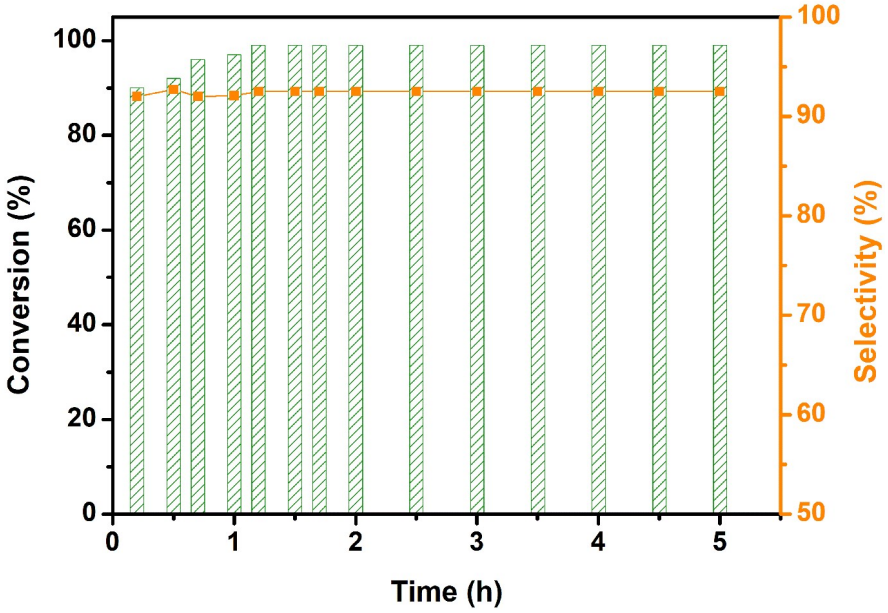

Figure S10. PW_{12}@rGO catalyzed epoxide ring-opening reaction in a continuous flow mode in the first 5 h.

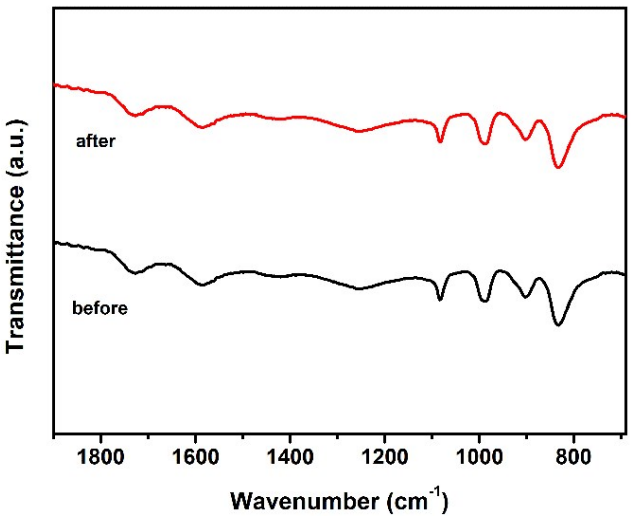

Figure S11. FT-IR spectra of PW_{12}@rGO before and after the continuous flow catalysis.

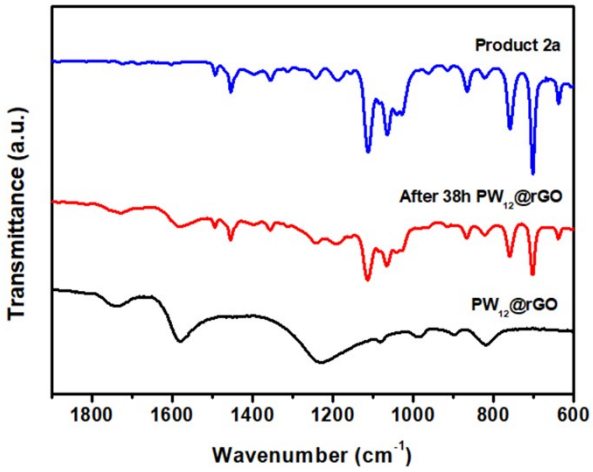

Figure S12. FT-IR spectra of fresh PW_{12}@rGO, product 2a, and PW_{12}@rGO after 38 hours' reaction.

Table S1. Surface acidities of PW_{12}@rGO determined by potentiometric titration with n-butylamine.

Sample	E_i (mV)	Acid amount (mmol n-butylamine g^{-1})
rGO	59	0.25
2.3wt% PW_{12}@rGO	499	1.48
3.6wt% PW_{12}@rGO	551	1.96
4.7wt% PW_{12}@rGO	566	2.47

Table S2. Comparison of heterogeneous catalysts for methanolysis of epoxide ring-opening reactions.

Catalyst	mole% catalyst versus styrene oxide	Temp. (℃)	Time (h)	Conv. (%)	TOF (h^{-1})	Ref.
MIL-101(HPW)	0.7	40	0.33	99.8	98.5	[1]
CuO / SiO_2	0.5	60	8.5	97	21.9	[2]
$PANF_{DTA}$@Fe(III)	5	RT	1	＞99	-	[3]
MIL-101-NH_2-PC-Ru(III)	0.1	RT	30	100	2325	[4]
Co-POM@MIL-101	0.1	RT	0.5	100	1504	[5]
PW_{12}@rGO	0.066	RT	0.17	99	8932	This work

References

1. L. H. Wee, F. Bonino, C. Lamberti, S. Bordiga and J. A. Martens, *Green Chem.*, 2014, **16**, 1351-1357.
2. F. Zaccheria, F. Santoro, R. Psaro and N. Ravasio, *Green Chem.*, 2011, **13**, 545.
3. X.-L. Shi, B. Sun, Q. Hu, Y. Chen and P. Duan, *Green Chem.*, 2019, **21**, 3573-3582.
4. A. K. Jafari, R. Kardanpour, S. Tangestaninejad, V. Mirkhani, M. Moghadam, I. Mohammadpoor-Baltork and F. Zadehahmadi, *J. Iran. Chem. Soc.*, 2018, **15**, 997-1006.
5. A. Marandi, S. Tangestaninejad, M. Moghadam, V. Mirkhani, A. Mechler, I. Mohammadpoor-Baltork and F. Zadehahmadi, *Appl. Organometal. Chem.*, 2017, **32**. e4065.